

# A Computational Fluid Dynamics Study on Improving Raw Fuel Injection Distributions in Front of Diesel Oxidation Catalysts

Watcharin Chantarasuwan\* and Ekathai Wirojsakunchai

## ABSTRACT

To increase the conversion efficiency of the exhaust gas in the advanced catalytic converters of modern diesel engines, the raw fuel injection technique (injecting diesel fuel in front of the catalytic converter) is introduced for raising exhaust temperatures to achieve emission reductions. When implementing this technique, special care is required as the flow distribution of the injected fuel droplets must be uniformly distributed to ensure the uniformity of internal temperatures across the cross sectional area of the catalytic converter. If a hot spot occurs inside due to uneven flow and the internal temperature exceeds the melting point of the substrate, this may cause substrate cracking which leads to failure of the device.

The current study aimed to apply a computational fluid dynamics program to explore the possibility of improving flow distributions of fuel droplets injected in front of the catalytic converter installed on the tested engine's exhaust system. Based on the literature, two methods—namely, a baffle and an extended pipe—were introduced and compared to the original exhaust system configuration.. The study also took into account the back pressure, the temperature distribution and the conversion efficiency of the exhaust gas within the catalytic converter. The results of the simulation showed that the flow/temperature distributions and the emission reductions were significantly improved by using these two methods. The baffle gave the best result. However, the drop in back pressure was also increased due to the complexity of its structure but was still under the design criteria.

**Keywords:** diesel oxidation catalyst, raw fuel injection, catalytic converter, baffles, computational fluid dynamics

## INTRODUCTION

As a result of the rise in oil prices in world markets, people prefer to use alternative fuels such as biodiesel, compressed natural gas (CNG), and liquid petroleum gas. However, these choices must take into account various aspects of the vehicle such as fuel consumption, engine performance and the emission of pollutants from the engine that must be in compliance with the law.

One option is to use natural gas which is currently much cheaper in Thailand. A diesel dual fuel (DDF) engine is one that combines diesel fuel with natural gas. The advantage of this type of engine is that the performance of the engine is comparable to a diesel engine and in addition, the nitrogen oxides ( $\text{NO}_x$ ) and soot emissions are low (Aroonsrisopon *et al.*, 2009; Wannatong *et al.*, 2009). The disadvantage of a DDF engine is that more hydrocarbon ( $\text{C}_3\text{H}_6$ ) and methane ( $\text{CH}_4$ )

are emitted (Karim *et al.*, 1993; Wannatong *et al.*, 2007, 2009).  $C_3H_6$  and  $CH_4$  can be eliminated via a catalytic converter but a proper exhaust gas temperature is required (Chiew *et al.*, 2005; Wirojsakunchai *et al.*, 2009).

However, under some conditions, the temperature of the exhaust gas is relatively low. A diesel oxidation catalyst (DOC) is unable to reach the light-off temperature of methane (Moallemi *et al.*, 1999; Wirojsakunchai *et al.*, 2009). In such a case, an increase in the temperature of the exhaust gas is required which, in turn, can raise the temperature of the catalytic converter to a suitable heat to treat the methane. A raw-fuel injection system has been used in many past works to increase the temperature of catalytic converter (Wirojsakunchai *et al.*, 2009; Noipeng *et al.*, 2011). When an injector was installed between the turbocharger and the catalytic converter to deliver diesel fuel to enhance the exothermic reaction in the catalytic converter,  $C_3H_6$  (in this case, a representative of the diesel fuel) and  $CH_4$  will oxidize with oxygen ( $O_2$ ) in the catalytic converter and be converted into carbon dioxide ( $CO_2$ ) and water ( $H_2O$ ) (Wirojsakunchai *et al.*, 2009; Noipeng *et al.*, 2011).

However, one of the most important problems in implementing a raw fuel injection technique is the excessive amount of diesel fuel used due to the mal-distribution of diesel fuel in front of the catalyst. Heat released from the chemical reaction can cause a rapid increase in the exhaust temperature which, in turn, produces severe thermal stress in the catalytic converter. This phenomenon can cause substrate failures from melting or cracking or both (Grobler and Fuls, 2005; Zhan *et al.*, 2006).

The concept of improving the flow distribution of the exhaust gas before entering the catalytic converter is explored in detail in diesel particulate filter (DPF) technology. Soot contained in the exhaust gas when trapped non-uniformly in the DPF can cause uncontrolled regeneration which leads to DPF failure (Lee

and Rutland, 2012). Therefore, most of the investigations into DPFs have focused on ensuring flow uniformity in front of the DPF. In addition, the flow uniformity will help increase the catalytic conversion efficiency (Martin *et al.*, 1998). Two main approaches reported in the literature are modification of the shape of the exhaust pipe and the inlet cone (Ranalli *et al.*, 2004; Zhang *et al.*, 2005) or the installation of additional equipment within the exhaust pipe to help promote uniform flow distribution (Girard *et al.*, 2006; Hilden and Crelline, 2006; Zhan *et al.*, 2006).

This current research was undertaken in the following manner. First, the behavior of the distribution of the diesel fuel was studied after it was injected in front of the catalyst using an exhaust system with the current configuration of the tested vehicle. The results were compared to the experimental data via conventional kinetic setups and user-defined functions in the software package. After the model was validated, extensive studies were undertaken on improvements to the uniform distribution of the diesel fuel before entering the catalytic converter with various exhaust configurations.

## MATERIALS AND METHODS

### Experimental setup

The main focus of this research was the use of a DDF engine in conjunction with the raw fuel injection system to reduce  $CH_4$  emissions. The experimental setup of the raw fuel injection system is shown in Figure 1. More details of the engine setup are provided in Noipeng *et al.* (2010).

The raw fuel injector is located between the turbocharged system and the pre-catalytic converter (PRE-CAT). Diesel fuel is sprayed into the pipeline to increase the temperature in the PRE-CAT which is a Pt-based catalyst. The main catalytic converter is a Pt/Pd-based catalyst designed for treating  $CH_4$ . Since the main focus of this study was to explore the behavior of the fuel injection distribution in front of the catalyst,

only simulation of the PRE-CAT was performed. The specifications of the PRE-CAT are shown in Table 1.

The engine used was a four-cylinder, four-stroke turbocharged Toyota 2KD-FTV diesel engine (commonly known as a Toyota D4D). The CNG port fuel injection was added to deliver natural gas when operating in DDF modes. The

selected test conditions were at 2,400 rpm, Lambda 1.7 and an exhaust temperature of 290 °C. The concentrations of the engine outputs under these particular conditions are shown in Table 2.

### Simulation setup

A commercial software package called ANSYS FLUENT Flow Modeling Software (version 13; ANSYS Inc.; Canonsburg, PA, USA) was used to simulate the flow fields. The 3D computer-aided design (CAD) model was generated by a 3D-scanner (supported by PTT Research & Technology Institute, Ayutthaya, Thailand) and imported into the CATIA CAD software (version 5; Dassault Systèmes; Velizy-Villacoublay, France) for use in the simulation. Figure 2a shows the computational domain of the current study in ANSYS FLUENT. The model was based on the exhaust configurations of a 2KD-FTV Toyota engine. The conditions chosen to perform the simulation as recommended in the ANSYS FLUENT manual are shown in Table 3. Figures 2b and 2c demonstrate the model improvements proposed in the current study. Five baffles were installed in front of the catalyst in Case B (Hilden

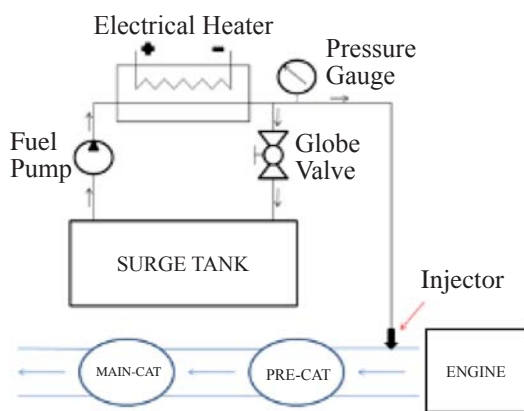


**Figure 1** Schematic diagram of raw fuel injection system after Noipeng *et al.* (2010). (MAIN-CAT = main catalytic converter, PRE-CAT = Pre-catalytic converter.)

**Table 1** Tested diesel oxidation catalyst (DOC) specifications.

Parameter	DOC (PRE-CAT)
CPSI	400
Cell Shape	Square
Substrate Volume (L)	1.96
Pt:Pd	1:0
PGM Loading (g.m <sup>-3</sup> )	854,332.42

PRE-CAT = Pre-catalyst, CPSI = Cells per square inch, PGM = Platinum Group Metals.

**Table 2** Test engine operating conditions and engine output concentrations.

Speed (rpm)	Lambda	Temperature (°C)	C <sub>3</sub> H <sub>6</sub> (ppm)	O <sub>2</sub> (%)	CO (ppm)
2,400	1.7	290	5,000	10.72	1,980

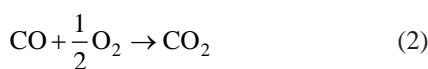
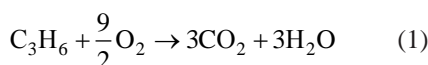
Rpm = Revolutions per minute, ppm = Parts per million.

and Crelline, 2006) to promote flow uniformity at the pipe bend. Case C was installed with the pipe length increased by 30 cm.

### Reaction kinetics for diesel oxidation catalyst models

Two kinetic model calculations—a volumetric reaction and a user-defined function (UDF)—were employed in the current study.

The volumetric reaction mechanism is a two-reaction model defined by Equations 1 and 2.



$C_3H_6$  and CO oxidations obey first order kinetics and the reaction rate can be expressed in the Arrhenius form as shown in Equation 3:

$$k = Ae^{-\frac{E_a}{RT}} \quad (3)$$

where  $k$  is the reaction rate (moles per cubic meter per second),  $A$  is the pre-exponent factor (moles per cubic meter per second),  $E_a$  is the activation energy ( $J.kmol^{-1}$ ),  $R$  is the ideal gas constant ( $8.314 J.K^{-1}.mol^{-1}$ ) and  $T$  is the temperature (Kelvin.)

The kinetics of the DOC aftertreatment using equations adopted from the literature (Koltsakis *et al.*, 1997; Koltsakis and Stamatelos, 1999) were implemented with the UDF. The reaction mechanism is a two-reaction model as shown in Equations (1) and (2). However, more advanced reaction rates of  $C_3H_6$  and CO, which are based on the Langmuir-Hinshelwood rate expressions are shown in Equations 4 and 5:

$$r_{co} = \frac{\left[ K_1 \cdot e^{-\frac{E_1}{T}} \cdot y_{CO} \cdot y_{O_2} \left[ 1 + K_2 \cdot e^{-\frac{E_2}{T}} \cdot y_{CO} + K_3 \cdot e^{-\frac{E_3}{T}} \cdot y_{C_3H_6} \right]^{-2} \right]}{\left[ 1 + K_4 \cdot e^{-\frac{E_4}{T}} \cdot y^2_{CO} \cdot y^2_{O_2} \right] \cdot \left[ 1 + K_5 \cdot e^{-\frac{E_5}{T}} \cdot y^{0.7}_{CO} \right] \cdot T_s} \quad (4)$$

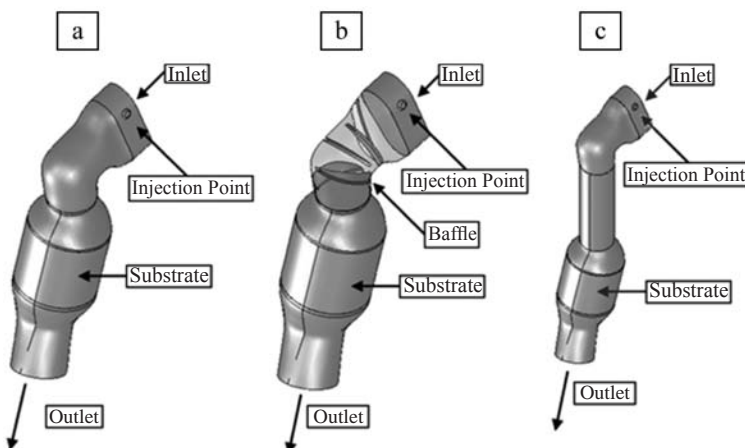


**Figure 2** Different structures of the pre-catalytic converter: (a) Standard outside equipment manufactured version, (b) Baffle included, (c) Increased length by 30 cm.

**Table 3** Details of model setup and boundary conditions for pre-catalytic converter.

Input		Boundary condition	
Type of mesh	Hexahedral and tetrahedral mesh	Mass-flow-inlet ( $kg.hr^{-1}$ )	103.87
Number of mesh	~750,000	Exhaust temperature ( $^{\circ}C$ )	290
Inlet, Outlet	Mass flow inlet, Pressure outlet	Wall temperature (K)	300
Turbulence	k- $\epsilon$ RNG	Pressure outlet ( $\Delta P$ )	0

k- $\epsilon$  RNG =  $k$  is an element of the re-normalisation group.

$$r_{C_3H_6} = \frac{\left[ K_1 \cdot e^{\frac{-E_1}{T}} \cdot y_{C_3H_6} \cdot y_{O_2} \right] \left[ 1 + K_2 \cdot e^{\frac{-E_2}{T}} \cdot y_{CO} + K_3 \cdot e^{\frac{-E_3}{T}} \cdot y_{C_3H_6} \right]^{-2}}{\left[ 1 + K_4 \cdot e^{\frac{-E_4}{T}} \cdot y^2_{CO} \cdot y^2_{C_3H_6} \right] \cdot \left[ 1 + K_5 \cdot e^{\frac{-E_5}{T}} \cdot y^{0.7}_{NO} \right] \cdot T_s} \quad (5)$$

where  $r$  is the reaction rate (moles per cubic meter per second),  $y_k$  is the mole fraction of species  $k$  in the gas phase (no unit),  $T_s$  is the solid temperature (Kelvin),  $E_1-E_5$  are the activation energy (Kelvin) and  $K_1-K_5$  are the frequency factors (no unit).

### Validation

In order to validate the simulation, tested conditions are shown in Table 2. Temperature and emission measurements were recorded at both the PRE-CAT inlet and outlet. A comparison of the temperature and the  $C_3H_6$  concentration between

the experiment and simulation are shown in Table 3. The results showing good agreement between the experiment and simulation are shown in Table 4. The values of calibrated  $A$  and  $E_a$  for both kinetic calculations can be found in Tables 5 and 6.

## RESULTS

Comparisons of the temperature at the outlets between the two kinetic models and the experiment are shown in Figure 4. Furthermore, temperature distributions are shown in Figure 5. When considering the temperature outlet, it was found that all three cases were similar regardless of the types of kinetic models employed. However,

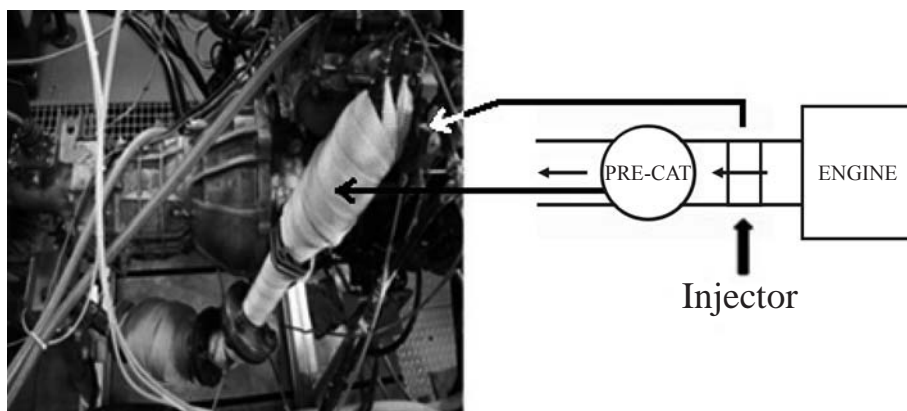


**Figure 3** Position of injector and pre-catalytic converter (PRE-CAT) in the experiment.

**Table 4** Comparison between the experimental and simulation results.

		Simulation	Experiment	% error
Volumetric	Temperature outlet (°C)	373	372	0.2
	$C_3H_6$ concentrate (ppm)	6634	5596	15.6
UDF	Temperature outlet (°C)	374	372	0.5
	$C_3H_6$ concentrate (ppm)	6515	5596	14.1

**Table 5** Kinetic oxidation of volumetric reaction used in the current study.

	Pre-exponential factor	Activation energy (J.kmol <sup>-1</sup> )
CO rate constant	2.239 E <sup>12</sup>	1.070 E <sup>04</sup>
$C_3H_6$ rate constant	4.836 E <sup>09</sup>	7.113 E <sup>04</sup>

when considering the temperature distribution for each kinetic model, it was clear that the best uniformly distributed flow occurred in case B, with case A having the worst because the maximum and minimum temperatures are different. As a result, case A can lead to higher thermal stress which might cause a crack when the substrate experiences high temperature exhausts.

The temperature distribution and the standard deviation of the temperature are shown in Figure 5. The more advanced kinetics from the UDF were clearly demonstrated by the better temperature distribution. A similar trend in the standard deviation was observed in both A and C.

Since a lower standard deviation indicates a better and more uniform flow distribution, case B clearly gave the best performance.

The conversion efficiency of  $C_3H_6$  in cases A, B and C for both kinetic calculations are shown in Figure 6. In terms of conversion efficiency, both kinetics gave very similar results. Figure 7 shows the  $C_3H_6$  distribution mole fraction of the substrate at the outlet. A uniform  $C_3H_6$  distribution mole fraction can be seen for Case B.

The results of the pressure drop in cases A, B and C are shown in Figure 8. Comparing case A to C, shows that increasing the length of

**Table 6** Kinetic oxidation of user-defined function used in the current study.

		Pre-exponential factor	Activation temperature (°C)	
CO Rate constant	$A_1$	74,074,000	$E_1$	4,615
	$A_2$	65.5	$E_2$	-961
	$A_3$	2,080	$E_3$	-361
	$A_4$	3.98	$E_4$	-11,611
	$A_5$	479,000	$E_5$	3,733
$C_3H_6$ Rate constant	$A_1$	$1.111 E^{09}$	$E_1$	8,285
	$A_2$	65.5	$E_2$	-961
	$A_3$	2,080	$E_3$	-361
	$A_4$	3.98	$E_4$	-11,611
	$A_5$	479,000	$E_5$	3733

$A_1$ – $A_5$  = Pre-exponential factor levels,  $E_1$ – $E_5$  = Activation temperature levels.

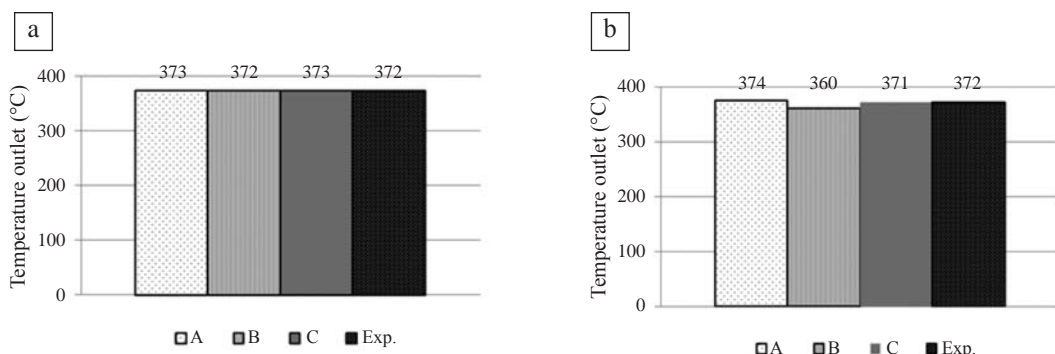


**Figure 4** Temperature outlet from: (a) Volumetric reaction and (b) User-defined function. (A = Original, B = Baffles, C = Increased length to 30 cm, Exp. = Experiment from Noipeng *et al.*, 2010).

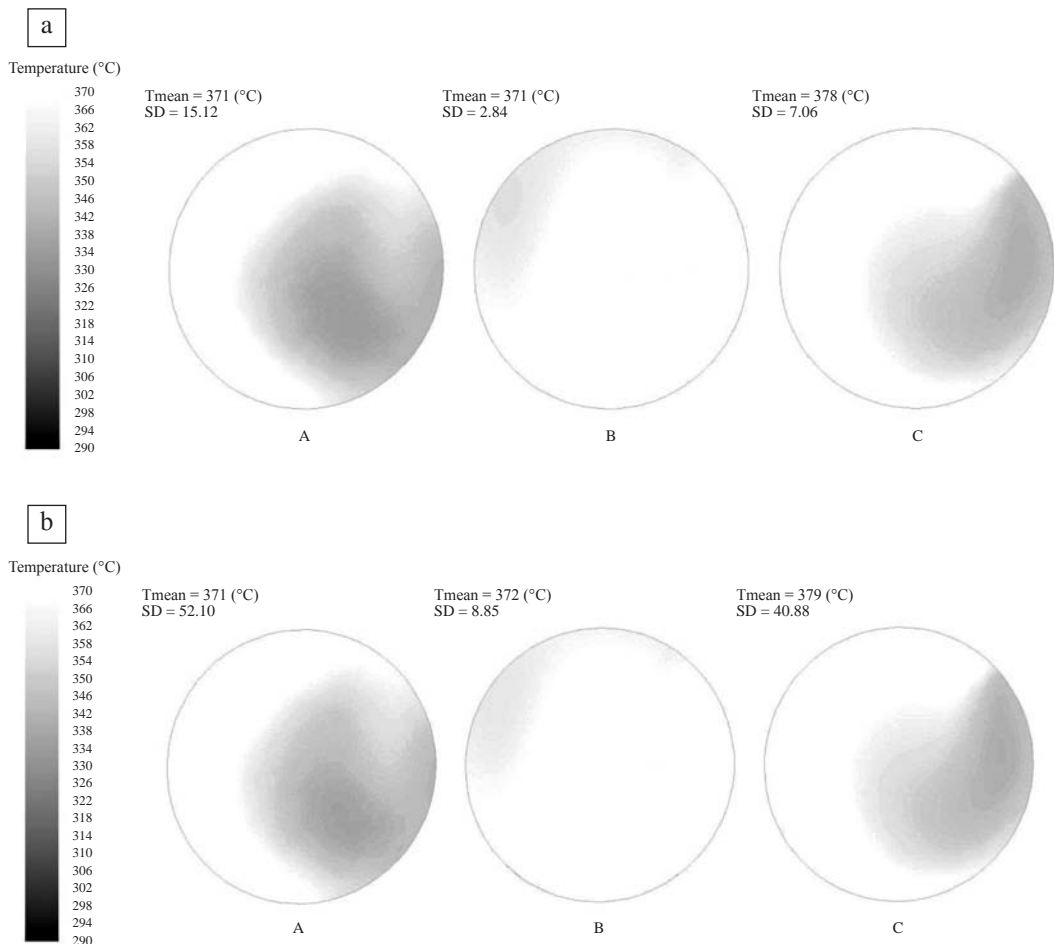


**Figure 5** Temperature distribution of cross section of substrate from volumetric reaction (5a–5c) and from user-defined function (5d–5f). (A = Original, B = Baffles, C = Increased length to 30 cm.)

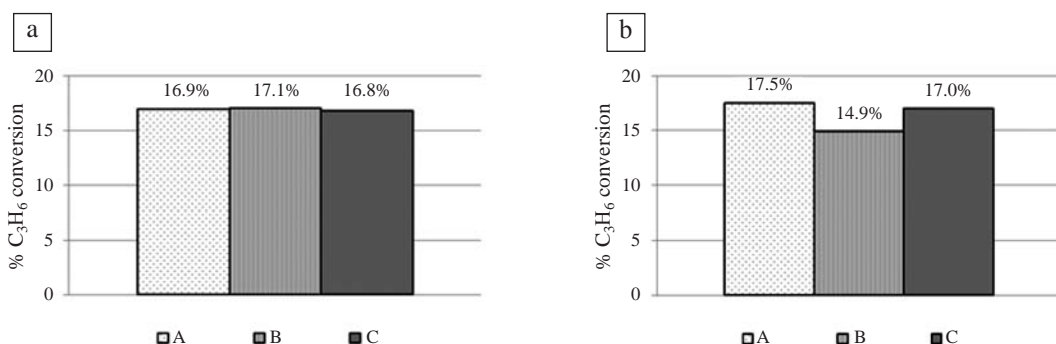


**Figure 6** %C<sub>3</sub>H<sub>6</sub> conversion from: (a) Volumetric reaction and (b) User-defined function. (A = Original, B = Baffles, C = Increased length to 30 cm.)

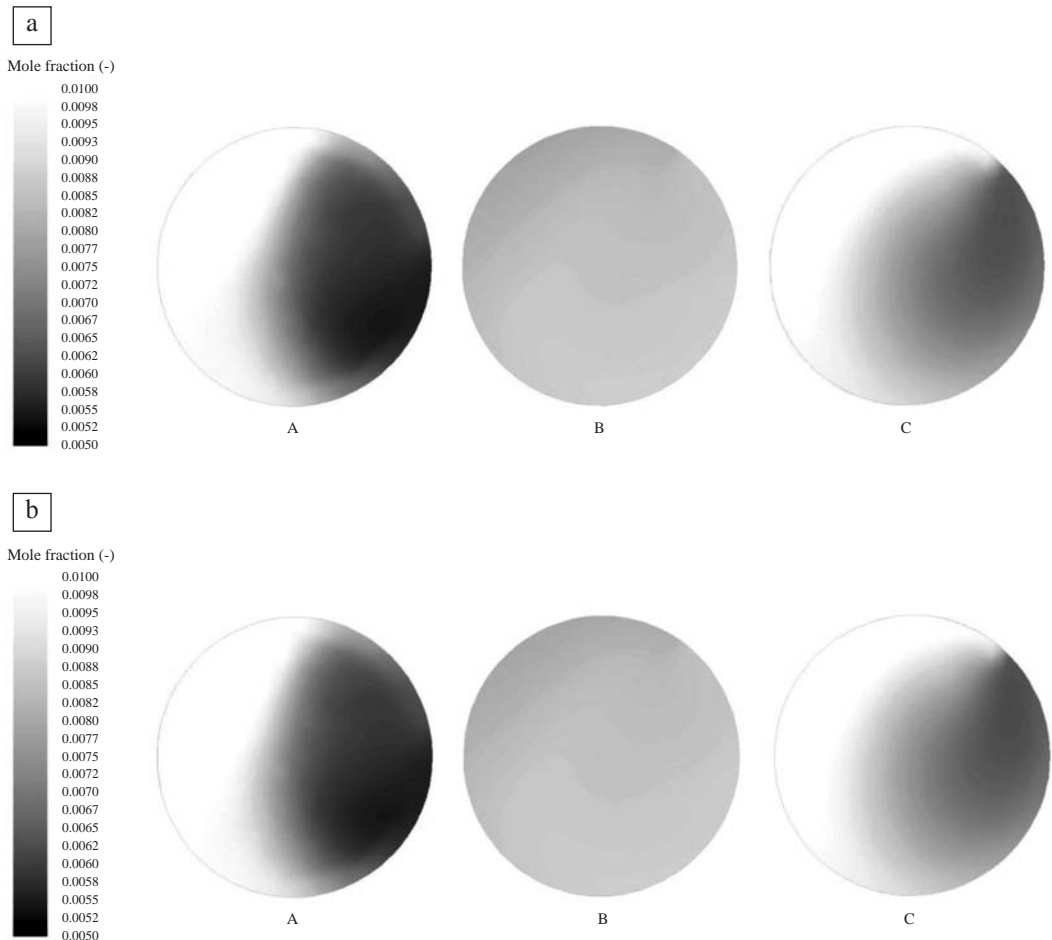


**Figure 7**  $\text{C}_3\text{H}_6$  distribution mole fraction of substrate at the outlet from (a) Volumetric reaction and (b) User-defined function. (A = Original, B = Baffles, C = Increased length to 30 cm.)

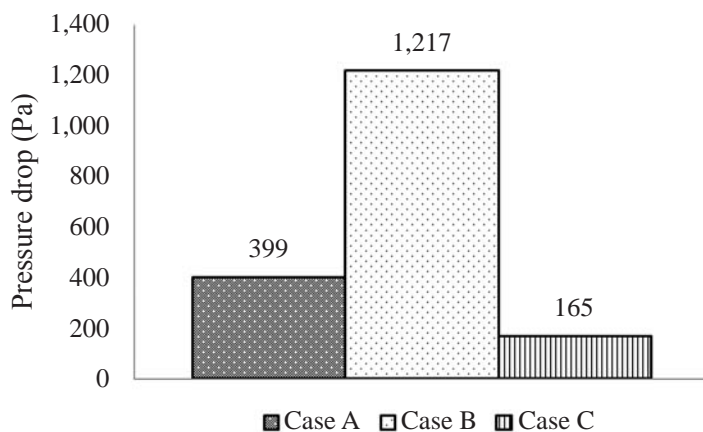


**Figure 8** Pressure drop at outlet for three cases studied.

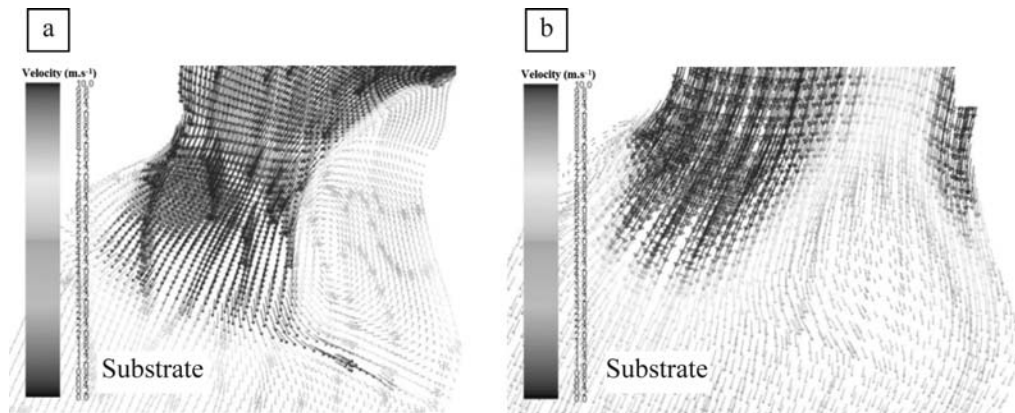


**Figure 9** Vortex of velocity profiles in front of the substrate: (a) Original and (b) Increased length to 30 cm.

the pipe in C helped to decrease the pressure drop because there was less vortex of velocity profiles generated in the bend of the pipe in front of the catalytic converter as seen in Figure 9. Comparing case A to B, the obstruction in the flow due to the installation of the baffles in B resulted in a high pressure drop. However the pressure drop was still acceptable for most aftertreatment applications (Hield, 2011).

## CONCLUSION

Two modified exhaust systems were intensively studied to improve the flow distribution of a raw fuel injection technique by controlling the exhaust gas emitted from a DDF engine. Two kinetic calculations were also implemented in the models. The conclusions from this study are: 1) the temperature outlet and the  $C_3H_6$  conversion efficiency in all cases was similar regardless of the kinetic models employed; 2) case B gave the best temperature distribution and with the more advanced kinetic calculations, the uniformity of the temperature distribution could be clearly seen; and 3) the pressure drop in case B was the highest due to its complex geometry, while cases A and C gave a lower pressure drop and vortex due to the extended length of pipe that helped to provide a more uniform flow.

## ACKNOWLEDGEMENTS

The author is sincerely thankful to the PTT Public Company Limited for their financial support throughout the course of this work. Mr. Ekkawut Pattarajaree is specially thanked for helping in the Optical Scan 3D and CAD program training.

## LITERATURE CITED

Aroonsrisopon, T., M. Salad, E. Wirojsakunchai, K. Wannatong, S. Siangsanorh and N. Akarapanjavit. 2009. Injection strategies for operational improvement of diesel dual fuel engines under low load conditions. *In Powertrains, Fuels and Lubricants Meeting*. 15 June 2009. Florence, Italy. SAE Technical Paper (2009-01-1855).

Chiew, L., P. Kroner and M. Ranalli. 2005. Diesel vaporizer: An innovative technology for reducing complexity and costs associated with DPF regeneration. *In SAE 2005 World Congress & Exhibition*. 11 April 2005. Detroit, Michigan, USA. SAE Technical Paper (2005-01-0671).

Girard J.W., F. Lacin, C.J. Hass and J. Hodonsky. 2006. Flow uniformity optimization for diesel aftertreatment systems. *In SAE 2006*

**World Congress & Exhibition.** 3 April 2006. Detroit, Michigan, USA. SAE Technical Paper (2006-01-1092).

Grobler, J.H. and P. Fuls. 2005. Impact of core face angle on maximum core temperature of a DPF at low flow rates. *In SAE 2005 World Congress & Exhibition.* 11 April 2005. Detroit, Michigan, USA. SAE Technical Paper (2005-01-0959).

Hield, P. 2011. **The Effect of Back Pressure on the Operation of a Diesel Engine.** Technical Report (DSTO-TR-2531). Defence Science and Technology Organisation. Australia.

Hilden, D.L. and C.C. Crelline. 2006. **Diesel Exhaust Aftertreatment Device Regeneration System.** US Patent 7,021,047.

Karim, G.A., Z. Liu and W. Jones. 1993. Exhaust emissions from dual fuel engines at light loads. *In International Fuels & Lubricants Meeting & Exposition.* 18 October 1993. Philadelphia, Pennsylvania, USA. SAE Technical Paper (932822).

Koltsakis G.C. and A.M. Stamatelos. 1999. Modeling dynamic phenomena in 3-way catalytic converters. **Chemical Engineering Science** 54: 4567–4578.

Koltsakis G.C., P.A. Konstantinidis and A.M. Stamatelos. 1997. Development and application range of mathematical model for 3-way catalysts. **Appl. Catal. B.** 12: 167–191.

Lee, H. and C.J. Rutland. 2012. Modeling uncontrolled regeneration of diesel particulate filters, taking into account hydrocarbon slip. **Proceedings of the Institution of Mechanical Engineers, Part D: Journal of Automobile Engineering** 227(2): 281–296.

Martin A.P., N.S. Will, A. Bordet, P. Cornet, C. Gondoin and X. Mouton. 1998. Effect of flow distribution on emissions performance of catalytic converters. *In International Congress & Exposition.* 23 February 1998. Detroit, Michigan, USA. SAE Technical Paper (980936).

Moallemi, F., G. Batley, V. Dupont, T.J. Foster, M. Pourkashanian and A. Williams. 1999. Chemical modelling and measurements of the catalytic combustion of CH<sub>4</sub>/air mixtures on platinum and palladium catalysts. **Catalysis Today** 47: 235–244.

Noipeng, A., W. Chantarasuwan and E. Wirojsakunchai. 2010. Applying raw fuel injection technique for reducing methane in diesel dual fuel engine aftertreatment. **Journal of Research in Engineering & Technology** 7(4): 59–74.

Noipeng, A., N. Waitayapat, T. Aroonsrisopon, E. Wirojsakunchai, T. Thummadetsak and K. Wannatong. 2011. **Experimental Investigation of Applying Raw Fuel Injection Technique for Reducing Methane in Aftertreatment of Diesel Dual Fuel Engines Operating under Medium Load Conditions.** Technical Paper. SAE Technical Paper (2011-01-2093). [Available from <http://papers.sae.org/2011-01-2093/>]. [Sourced : 10 september 2013].

Ranalli, M., J. Klement, M. Hoehnen and R. Rosenberger. 2004. Soot distribution in DPF systems. A simple and cost effective measurement method for series development. *In SAE 2004 World Congress & Exhibition.* 8 March 2004. Detroit, Michigan, USA. SAE Technical Paper (2004-01-1432).

Wannatong, K., N. Akarapanyavit and S. Siengsanorh. 2007. **Combustion and Knock Characteristics of Natural Gas Diesel Dual Fuel Engine.** Technical Paper. SAE Technical Paper (2007-01-2047). [Available from <http://papers.sae.org/2007-01-2047/>]. [Sourced : 10 september 2013].

Wannatong, K., N. Akarapanyavit, S. Siengsanorh, T. Aroonsrisopon and S. Chanchaona. 2009. New diesel dual fuel concepts: Part load improvement. *In Powertrains, Fuels and Lubricants Meeting.* 15 June 2009. Florence, Italy. SAE Technical Paper (2009-01-1797).

Wirojsakunchai, E., T. Aroonsrisopon, K. Wannatong and N. Akarapanjavit. 2009. A simulation study of an aftertreatment system level model for diesel dual fuel (DDF) engine emission control. *In Powertrains, Fuels and Lubricants Meeting.* 15 June 2009, Florence, Italy. SAE Technical Paper (2009-01-1966).

Zhan, R., Y. Huang and M. Khair. 2006. Methodologies to control DPF uncontrolled regenerations. *In SAE 2006 World Congress & Exhibition.* 3 April 2006, Detroit, Michigan, USA. SAE Technical Paper (2006-01-1090).

Zhang, X., M. Romzek, M. Keck and F. Kurz. 2005. Numerical optimization of flow uniformity inside diesel particulate filters. *In Powertrain & Fluid Systems Conference & Exhibition.* 24 October 2005, San Antonio, Texas, USA. SAE Technical Paper (2005-01-3702).